Partial Differential Equation-Based Approach for Empirical Mode Decomposition: Application on Image Analysis

Oumar Niang, Abdoulaye Thioune, Mouhamed Cheikh El Gueirea, Eric Deléchelle, Jacques Lemoine

Partial Differential Equation-Based Approach for Empirical Mode Decomposition: Application on Image Analysis

Oumar Niang, Abdoulaye Thioune, Mouhamed Cheikh El Gueirea, Eric Deléchelle and Jacques Lemoine

***Abstract*—The major problem with Empirical Mode Decomposition (EMD) algorithm is its lack of a theoretical framework. So, it is difficult to characterize and evaluate this approach. In this paper, we propose in the two dimensional case, the use of an alternative implementation to the algorithmic definition of the so-called 'sifting process' used in the original Huang's Empirical Mode Decomposition method. This approach, especially based on Partial Differential Equations (PDE) was presented by O. Niang and al. in previous works, in 2005 and 2007 and lays on a nonlinear diffusion-based filtering process to solve the mean-envelope estimation problem. In 1D case, the efficiency of the PDE-based method, compared to the original EMD algorithmic version, is also illustrated in recent paper [1]. Recently, several bi-dimensional extensions for EMD method were proposed. Despite some efforts, 2D versions for EMD appear poorly performing and are very time consuming. So in this work, an extension to 2D space of the PDE-based approach is extensively described. This approach has been applied in case of both signal and image decomposition. Obtained results confirm the usefulness of the new PDE-based sifting process for decomposition of various kinds of data. Some results have been provided in the case of image decomposition. The effectiveness of the approach encourages its usage in a number of signal and image applications such as denoising, detrending, or texture analysis.**

***Index Terms*—Empirical Mode Decomposition (EMD), Mean-Envelope, Partial Differential Equation, Restoration, Signal, Image, Inpainting.**

I. Introduction

In complement of a previously published letter [1]–[3], this paper addresses an alternative to the problem of mean-envelope estimation of a signal that is a crucial step in the Empirical Mode Decomposition (EMD) method originally proposed by N.E. Huang et al. [4]. Although EMD is often remarkably effective in some applications [5]–[8], this method is faced with the difficulty of being essentially based on an algorithm, and therefore not admitting an analytical formulation which would permit a theoretical analysis and performance evaluation.

The purpose of this paper is therefore to contribute analytically to a better understanding of the EMD method with an 2D extension of the approach presented in [3]. There are various applications of nonlinear diffusion filtering in signal and image processing. Such filters are used for denoising, enhancement, gap completion, and are expected to play an increasing role in future applications. Nonlinear diffusion filtering is a continuous filter, formulated as a partial differential equation (PDE). The filter operation is practically performed by solving the nonlinear PDE numerically. In [2] a fully mathematical study of PDE model proposed in this paper was done. The paper is organized as follows: we recall the classical EMD and present the PDE model in sections II and III. Section IV recalls some models of diffusion equation used in image processing. Then the 2D extension of the PDE model for EMD is presented in Section V. We finish with numerical simulations and a conclusion.

II. Empirical Mode Decomposition Basics

We summarized in this section the EMD method. The literature on the EMD and its use in applied science is abundant, a permanent updating of some recent and not exhaustive developments may be obtained by consulting the following references. Details on the implementation of EMD algorithm and Matlab codes for some applications are fully available in [9]–[11].

A. EMD principle

EMD [4] method decomposes iteratively a complex signal (i.e. with several characteristic time scales coexisting) into elementary AM-FM type components called Intrinsic Mode Functions (IMF). The underlying principle of this decomposition is to locally identify in the signal, the most rapid oscillations defined as the waveform interpolating interwoven local maxima and minima. To do so, local maxima points (resp. local minima points) are interpolated with a cubic spline, to yield the upper (resp. lower) envelope. The mean envelope (half sum of upper and lower envelopes) is then subtracted from the initial signal, and the same interpolation scheme is re-iterated on the remainder. The so called sifting process stops when the mean envelope is

Oumar Niang is with the Département Génie Informatique et Télécommunications, Ecole Polytechnique de Thiès BP A 10 Thies, BP 64551 Dakar-Fann, Sénégal, and also with the Laboratoire Images, Signaux et Systmes Intelligents (LISSIE.A.3956) Université Paris Est Créteil Val-de-Marne, Créteil 94010, France and with the Laboratoire dAnalyse Numérique et dInformatique (LANI), Université Gaston Berger (UGB), Saint-Louis, Sénégal (e-mail: oniang@ucad.sn; niangom@yahoo.fr)

M. C. El Gueirea and A.Thioune are PhD Student respectively at UFR-SAT of Gaston Berger University and at Faculté des Sciences et Technique of the Cheikh Anta Diop University in Sénégal. BP 64551 Dakar Fann, Senegal. (e-mail: thiounelaye@yahoo.fr).

É. Delèchelle and J. Lemoine are with the Laboratoire Images, Signaux et Systèmes Intelligents (LiSSi-E.A.3956)-Université Paris Est Créteil Val-de- Marne, Créteil 94010, France (e-mail: lemoine@u-pec.fr,delechelle@u-pec.fr).

reasonably zero everywhere, and the resulting signal is called the first IMF. The higher order IMFs are iteratively extracted applying the same procedure to the initial signal after the previous IMFs have been removed.

To be an IMF, a signal must satisfy two criteria, the first one being that the number of local maxima and the number of local minima differ by at most one, and the second, the mean of its upper and lower envelopes equals zero. So, for any 1D discrete signal, EMD ends up with the following representation

$$s\left[n\right] = r_K\left[n\right] + \sum_{k=1}^{K} imf_k\left[n\right],$$

where imf_k is the k-th mode (or IMF) of the signal, and r_K stands for residual trend (a low order polynomial component).

Sifting procedure generate a finite (and limited) number of IMFs that seems nearly orthogonal to each other [4]. By nature of the decomposition procedure, the technique decomposes data into K fundamental components, each with distinct time scale: the first component has the smallest time scale. As the decomposition proceeds, the time scale increases, and hence, the mean frequency of the mode decreases.

B. EMD related works

Numerous efforts on EMD method were essentially done for algorithm improvement [12], experimental characterization on fractional Gaussian noise decomposition showing spontaneous emergence of a filter bank structure, almost dyadic and self-similar and resulting on a possible Hurst's exponent estimation [13]–[16].To decompose noised data or signal with intermittencies, two EMD improvements have been proposed in [17] by Ensemble EMD (EEMD) method with an multi-dimensionnal version in [18] , and in [1] with an Tykhonov regularization. After the introduction of complex signal EMD and the rotation invariant EMD proposed respectively in [19] and in [20], the Bivariate EMD in [21], the decomposition of multivariate signals using the Active Angle Averaging is presented in [22]. Several works have proposed different approaches for 2D extension of EMD, including a row-wise/column-wise decomposition, in the spirit of the so-called non-standard wavelet transform, or a truly bidimensional version of EMD [23]–[28]. A fully multivariate EMD method is presented in [29]. In [30], a multi-dimensional ensemble empirical mode decomposition (MEEMD) for multi-dimensional data (such as images or solid with variable density) is proposed. A first conclusion from these works is that, EMD method appears as a simple, local and fully data-driven approach, adapted to nonlinear oscillations. More, the combination of the EMD method and the associated Hilbert spectral analysis can offer a powerful method for nonlinear and non-stationary data analysis [4], [9], [10].

During sifting process, cubic splines interpolation is a crucial step to create the upper and lower envelopes of the data set. Fitting of the splines at the extrema can produce several inconveniences: (i) problems can occur near the ends; (ii) end swings can eventually propagate inward; (iii) overshoots and undershoots could occur, (iv) influence of the sampling [32]. Some solutions were proposed in [33], [34]. In 2D versions, the main drawbacks of EMD are the definition of extrema of an image (or a surface), and the choice of the interpolation method acting on a set of scattering points. More, such decomposition in 2D is extremely time-consuming.

Some contributions for theoretical understanding of the EMD should be noted. Daubaucies and al. [35] proposed an combination of wavelet analysis and reallocation method and introduce a precise mathematical denition for a class of functions that can be viewed as a superposition of a reasonably small number of approximately harmonic components. Globally EMD method suffers from the drawback of a lack of mathematical framework beyond numerical simulations. Despite some works [1]–[3], [36], [37], a complet EMD formalism remains a challenge. In the following section, we recall the analytical contribution of O. Niang and al. in [1]–[3] based on PDE approach to compute the mean enveloppe.

III. PDE-Based Formulation in 1-D

The mathematical modeling leads to a PDE parabolic system which gives a family of solutions that interpolate the charcacteristic points of a signal. This family of functions converge to the envelope of the signal which was calculated by cubic spline interpolation in classical EMD. It is proven that this solution is in $H^2(\Omega)$ whereas the input signal representing the initial solution of the PDE is in $H^1(\Omega)$, with Ω is an closed and bounded set signal which is the domain of the signal. A possible form for fourth order diffusion equation introduced in [3] and in [2] is:

$$\frac{\partial s\left(x,t\right)}{\partial t} = -\frac{\partial}{\partial x}\left(g(x,t)\frac{\partial^3 s\left(x,t\right)}{\partial x^3}\right), \tag{1}$$

where $g(x,t)$ is the diffusivity function possibly depending on both position and time, and where the time variable is artificial, and measures the degree of processing (e.g. smoothing) of the signal. Equation (1) can be viewed as a Long-Range Diffusion (LRD) equation (see for example reference [38, p.244]), with thresholding function $g(x)$ depending only on position (constant in time) and more precisely on some characteristic fix points of the signal to decompose. After derivation equation (1) read:

$$s_t\left(x,t\right) = -\partial_x^1 g(x)\partial_x^3 s\left(x,t\right), \tag{2}$$

where the subscript t denotes partial differentiation with respect to the variable t and ∂_x^q denotes partial differentiation of order q with respect to the variable x. In the following we use the notation $s_0(x) = s(x, t = 0)$ for initial condition and $s_\infty(x) = s(x, t = \infty)$ for asymptotic solution of equation (1).

In order to implement sifting procedure in a PDE-based framework, the following processes are based on the definition of characteristic fix points of a function: (i) turning-points; (ii) curvature-points. Here, we are interested in turning points

that are minima, maxima and inflexion points, defining by the values of their first and/or second derivatives. With this model, to estimate lower and upper envelopes, a couple of PDE is given instead of a cubic spline inerpolation in sifting process.

A. A coupled PDEs system

A simple method to estimate mean-envelope is to formulate a coupled PDEs system to mimic Huang's sifting process based on upper and lower envelopes estimation. Turning points are here respectively maxima and minima of the signal to be decomposed. This coupled PDEs system, based on equation (1) leads to (see also [2], [3] for a more less general PDE formulation):

$$\begin{cases} s_t^+(x,t) = -\delta_x^1\left[g^+\left(\delta_x^1 s_0(x), \delta_x^2 s_0(x)\right)\delta_x^3 s^+(x,t)\right] \\ s_t^-(x,t) = -\delta_x^1\left[g^-\left(\delta_x^1 s_0(x), \delta_x^2 s_0(x)\right)\delta_x^3 s^-(x,t)\right] \end{cases} \tag{3}$$

After convergence of system (3) [2],asymptotic solutions $s_\infty^+(x)$ and $s_\infty^-(x)$ stand respectively for upper and lower envelops of signal s_0. Hence, mean-envelope of s_0 is obtained by:

$$s_\infty(x) = \tfrac{1}{2}\left[s_\infty^+(x) + s_\infty^-(x)\right].$$

In equation (3), stopping functions, $g^\pm$, depend on both first and second order signal derivatives, with $0 \leq g^\pm \leq 1$. For example, a good choice for stopping functions seems (according to our tests) to be

$$g^\pm(x) = \tfrac{1}{9}\left[\left|sgn\left(\delta_x^1 s_0(x)\right)\right| \pm sgn\left(\delta_x^2 s_0(x)\right) + 1\right]^2. \tag{4}$$

In such a way, $g^+ = 0$ and $\delta_x^1 g^+ = 0$ at maxima of s_0, in the same way $g^- = 0$ and $\delta_x^1 g^- = 0$ at minima of s_0. So, LRD acts only between two consecutive maxima (resp. minima) points until fourth-order derivative of $s(x,t)$ is canceled. Since, stopping functions are piecewise constant, after convergence the resulting signal $s_\infty^+(x)$ (resp. $s_\infty^-(x)$) is a piecewise cubic polynomial curve interpolating the successive maxima (resp. minima) of signal. In equation (4) sign function, $sgn(z)$, is replaced by a regularized version. A possible expression is given by $sgn_\alpha(z) = 2/\pi \arctan(\pi z/\alpha)$.
Physically the PDE solution diffuse everywhere except on the extrema of the signal. Its smoothing effect works like in the selective diffusion equation case.

B. Interpolation with tension

A more general form for equation (2) is

$$s_t(x,t) = \delta_x^1\left[g(x)\left(\alpha\delta_x^1 s(x,t) - (1-\alpha)\delta_x^3 s(x,t)\right)\right], \tag{5}$$

so, in this form, α is the tension parameter, and ranges from 0 to 1. Zero tension, $\alpha = 0$, leads to the biharmonic equation form (2) and corresponds to the minimum curvature construction for upper and lower envelopes. The case $\alpha = 1$ corresponds to infinite tension (piecewise linear envelopes).

C. Numerical resolution

Numerical resolution for coupled PDEs system based on equation (5) with Neumann boundaries conditions, is implemented with a Crank-Nicolson scheme (semi or fully implicit) or Du Fort and Frankel scheme. Noting that a particular attention is made for derivatives of s_0 in the defintion of $g(x)$:

$$g(x) = g\left(D_1 s_0(x), D_2 s_0(x)\right),$$

where $g = g^\pm$, and $D_1 z = minmod(D^+ z, D^- z)$, $D_2 z = D^+ D^-$, where D^+ and D^- are forward and backward first difference operators on the x-dimension, and where $minmod(a,b)$ stands for the minmod limiter $minmod(a,b) = \frac{1}{2}[sgn(a) + sgn(b)] \cdot min(|a|,|b|)$.
In the next paragraph, before presenting a 2D version of PDE-based approach for EMD, we recall some models of diffusion equations in image processing.

IV. Diffusion Equations for Image Processing

This part consists on a brief and non exhaustive presentation of classical nonlinear diffusion filters for image processing.

A. Perona-Malik equation

Let us first provide a model for nonlinear diffusion in image filtering. We briefly describe the filter proposed by Catté, Lions, Morel and Coll [39]. This filter is a modified version of the well know Perona and Malik model [40]. The basic equation that governs nonlinear diffusion filtering is:

$$u_t(\mathbf{x},t) = div\left(g\left(\left|\nabla u(\mathbf{x},t)\right|^2\right)\nabla u(\mathbf{x},t)\right), \tag{6}$$

with $\mathbf{x} = (x_1, x_2)$, and where $u(\mathbf{x},t)$ is a filtered version of the original image $u(\mathbf{x},t) = u_0(\mathbf{x})$ as the initial condition, and with reflecting boundary. In equation (6) $g(\cdot)$ is the conductivity (or diffusivity) function, which dependent (in space and time) on the image gradient magnitude. Several forms of diffusivity were introduced in the original paper of Perona and Malik [40]. All forms of diffusivity are chosen to be a monotonically decreasing function of the signal gradient. This behavior implies that the diffusion process maintains homogenous regions since little smoothing flow is generated for low image gradients, and in the same way, edges are preserved by a small flow in regions where the image gradients are high. Possible expressions for conductivity functions are:

$$\begin{aligned} g_1(\mathbf{x},t) &= \frac{1}{1 + \left(\frac{|\nabla u(\mathbf{x},t)|}{\beta}\right)^2}, \\ g_2(\mathbf{x},t) &= \exp\left(-\left(\frac{|\nabla u(\mathbf{x},t)|}{\beta}\right)^2\right). \end{aligned} \tag{7}$$

Parameter β is a threshold parameter, which influences the anisotropic smoothing process. The nonlinear equation (6) acts as a forward parabolic equation smoothing regions while preserving edges. In the Backward diffusion filters, a different approach is taken. Its goal is to emphasize large gradients and can be viewed as a reversing diffusion process. The moving back in time can be obtained mathematically by changing the sign of the conductivity function.

Other methods based on high order PDE are provided for image restoration like in [41]–[43]. With these methods, different functionals can be used to measure the oscillations in an image and a general formulation of the noise removal problem is solved by optimisation with constraint on noise level. Most numerical schemes for diffusion process implementation produce instability, oscillations, or noise amplification, or converge to a trivial solution like the average value of the whole gray level image values. So, in order to implement an appropriate stopping mechanism and to overcome stability problems, various modifications of the original diffusion scheme were attempted. Efficient numerical schemes were introduced in [44] based on Additive Operator Splitting (AOS) schemes, or based on Alternating Direction Implicit (ADI) scheme. See [44]–[47] for a review and extensions of these methods. Unlike these methods of high order PDE that are specially developed for denoising, our model was constructed to interpolate the characteristic points of a signal. The PDE interpolator is not based on any a priori knowledge constraint on the noise level as opposed to Total Variation method in [43].

B. Selective image smoothing problem

Contrary to linear diffusion filters - signal convoluted with Gaussian of varying widths - nonlinear diffusion filters are possible solution to solve the selective image-smoothing problem. The major problem of nonlinear diffusion-based process is that it is generally difficult to correctly separate the high frequency components from the low frequency ones. A possible way is to adopt a dyadic wavelet-based approximation scheme [48]. Under this framework, a signal is decomposed into high frequency components and low frequency ones by using wavelet approximated high-pass and low-pass filters. In case of denoising applications, the objective of this process is to use the diffusivity function as a guide to retain useful data and suppress noise.

In the past few years, a number of authors have proposed fourth order PDEs for image smoothing and denoising with the hope that these methods would perform better than their second order analogues [49]–[54]. Indeed there are good reasons to consider fourth order equations. First, fourth order linear diffusion damps oscillations at high frequencies (i.e. noise) much faster than second order diffusion. Second, there is the possibility of having schemes that include effects of curvature (i.e. the second derivatives of the image) in the dynamics, thus creating a richer set of functional behaviors. On the other hand, the theory of fourth order nonlinear PDEs is far less developed than the second order analogues. Also such equations often do not satisfy a maximum principle or comparison principle, and implementation of the equations could thus introduce artificial singularities or other undesirable behavior. In recent studies, Tumblin [55], Tumblin and Turk [52] and Wei [53] proposed equations of the form:

$$u_t\left(\mathbf{x},t\right) = -div\left(g\left(m\left(u\right)\right)\nabla\Delta u\left(\mathbf{x},t\right)\right), \tag{8}$$

where $g(\cdot) = g_1(\cdot)$ as in equation (7), and m is some measurement of $u(\mathbf{x},t)$. In [52], equation (8) is called a 'Low Curvature Image Simplifier' (LCIS), and a good choice for m is defined as $m = \Delta u$ to enforce isotropic diffusion [55].

C. Super diffusion model

In fact, equation (6) is a more general form of the diffusion equation derived from Fick's law for mass flux, $\mathbf{j}_1$,

$$u_t(\mathbf{x},t) = -div\left(\mathbf{j}_1\left(\mathbf{x},t\right)\right),$$

with $\mathbf{j}_1\left(\mathbf{x},t\right) = -G_1\nabla u\left(\mathbf{x},t\right)$, where G_1 being a constant. From a point of view of kinetic theory, this is an approximation of a quasi homogeneous system which is near equilibrium. A better approximation can be expressed as a super flux of order Q

$$\mathbf{j}_Q\left(\mathbf{x},t\right) = \sum_{q=1}^{Q}\left(-1\right)^q G_q\left(\mathbf{x},t\right)\nabla\nabla^{2q-2}u\left(\mathbf{x},t\right),$$

with $Q = 1, 2, \ldots$, and where G_q ($q > 1$, $G_q \geq 0$) describe super diffusivity functions. A truncation at the second order super flux, $\mathbf{j}_2$, leads to the expression

$$u_t(\mathbf{x},t) = -div\left(-G_1\nabla u\left(\mathbf{x},t\right) + G_2\nabla\Delta u\left(\mathbf{x},t\right)\right). \tag{9}$$

A more simple expression for $u_t(\mathbf{x},t)$ is:

$$u_t\left(\mathbf{x},t\right) = -\sum_{q=1}^{Q}\left(-1\right)^q G_q\left(\mathbf{x},t\right)\nabla^{2q}u\left(\mathbf{x},t\right).$$

For $Q = 2$, we have:

$$u_t\left(\mathbf{x},t\right) = G_1\left(\mathbf{x},t\right)\Delta u(\mathbf{x},t) - G_2\left(\mathbf{x},t\right)\Delta^2 u(\mathbf{x},t). \tag{10}$$

These PDE tools for digital image processing make more reachable the 2D extension of the 1D PDE-based method for EMD.

V. PDE-Based Bidimensional Empirical Mode Decomposition

In this part, we develop an extension in 2D space of the proposed 1D PDE-based sifting process in order to perform Bidimensional Empirical Mode Decomposition (BEMD).

A. Proposed super diffusion model in 2D-space

We consider here equation (5), with diffusion matrix functions, $\mathbf{G}_q$, as

$$\mathbf{G}_q(\mathbf{x}) = \begin{pmatrix} g_{q,1}(\mathbf{x}) & 0 \\ 0 & g_{q,2}(\mathbf{x}) \end{pmatrix},$$

where $g_{q,i}$ is the stopping function for qth-order term in the direction i.
The proposed super diffusion equation then leads to, for $Q = 2$ and with tension parameter:

$$u_t(\mathbf{x},t) = div\left(\alpha\,\mathbf{G}_1\nabla u\left(\mathbf{x},t\right) - \left(1-\alpha\right)\mathbf{G}_2\nabla\Delta u\left(\mathbf{x},t\right)\right). \tag{11}$$

In order to estimate upper and lower envelopes, functions $g_{q,i}$ in $\mathbf{G}_q$ must to be specified. Obviously, there are many ways to construct anisotropic diffusion functionals in 2D. For simplicity, we test the following choice, with $\mathbf{G}_1 = \mathbf{G}_2$, which is based on definition (4), for all $q = 1, 2$:

$$g_{q,i}^{\pm}\left(\mathbf{x}\right) = \tfrac{1}{9}\left[\left|sgn\left(\delta_{x_i}^1 u_0\right)\right| \pm sgn\left(\delta_{x_i}^2 u_0\right) + 1\right]^2. \tag{12}$$

In equation (12) signs $\pm$ stand respectively for stopping functions for upper and lower envelopes estimation.

B. Relation with PDEs defined on implicit surfaces

We can make the relationship of this simple LRD equation with a $2qth$-order heat equation on a curve or surface S in $\mathbb{R}^N$ ($N = 2$ for a curve and $N = 3$ for a surface), which is given by

$$u_t(\mathbf{x}, t) = -(-1)^q \nabla_S^{2q} u(\mathbf{x}, t), \tag{13}$$

with initial condition $u(\mathbf{y}, 0) = f$ for $\mathbf{y}$ on S. Here, $\nabla_S^{2q} u$ is the $2q$-order differential operator applied on u intrinsic to the surface S. If S is defined as an implicit surface from a level set function ϕ, i.e. S is defined as the zero level set of ϕ, $S = \left\{\mathbf{x} \in \mathbb{R}^{\mathbf{N}} : \phi(\mathbf{x}) = \mathbf{0})\right\}$. So, it is easy to show that for all point on S, Laplacian operator $\Delta_S u$ intrinsic to S can be compute using extrinsic derivatives as

$$\Delta_S u(\mathbf{x}) = \frac{1}{|\nabla\phi(\mathbf{x})|} \nabla \cdot (\mathbf{P}(\mathbf{x}) \nabla u(\mathbf{x}) |\nabla\phi(\mathbf{x})|), \tag{14}$$

where $\mathbf{P}$ is a projection operator. If ϕ is a signed distance function, then $|\nabla\phi(\mathbf{x})| = 1$, then equation (14) reduce to

$$\Delta_S u(\mathbf{x}) = \nabla \cdot (\mathbf{P}(\mathbf{x}) \nabla u(\mathbf{x})).$$

In the same manner, we can define biharmonic operator, Δ_S^2 on u intrinsic to S as

$$\Delta_S^2 u(\mathbf{x}) = \nabla \cdot (\mathbf{P}(\mathbf{x}) \nabla (\nabla \cdot (\mathbf{P}(\mathbf{x}) \nabla u(\mathbf{x})))).$$

As an example, letting S be the line making angle θ with the x_1-axis in the image plane $\mathbf{x} = (x_1, x_2)$. The projection matrix is then define by

$$\mathbf{P} = \begin{pmatrix} a & c \\ c & b \end{pmatrix} = \begin{pmatrix} cos^2\theta & cos\theta sin\theta \\ cos\theta sin\theta & sin^2\theta \end{pmatrix}.$$

Noting that $\mathbf{P}$ not depends on $\mathbf{x}$ for this example, the second and fourth order heat equations on S, $q = 1, 2$ in equation (13), are given by

$$u_t = -(-1)^q \left(a^q \, \partial_{x_1}^{2q} u + 2c^q \, \partial_{x_1}^q \partial_{x_2}^q u + b^q \, \partial_{x_2}^{2q} u\right).$$

C. Numerical resolutions

Many schemes are proposed for performing nonlinear diffusion filtering in 2-dimensional space. See [47] for an extended review. For purpose of simplicity, we consider here numerical resolution schemes for fourth-order PDE with no tension ($\alpha = 0$) in equation (11).

Explicit scheme. To approximate PDE-based sifting process numerically, we replace the derivatives by finite differences. Since continuous fourth-order PDE has the structure

$$u_t = -\sum_{i,j=1}^{2} \partial_{x_i}^1 \left(g_i \partial_{x_i}^1 \partial_{x_j}^2 u\right), \tag{15}$$

its simplest discretization, between iterations k and $k+1$, is given by the difference scheme

$$\frac{U^{k+1} - U^k}{\Delta t} = -\sum_{i,j=1}^{2} L_{ij} U^k,$$

so,

$$U^{k+1} = \left(I - \Delta t \sum_{i,j=1}^{2} L_{ij}\right) U^k, \tag{16}$$

where U is the vector formed with the values at each pixel of $u(\mathbf{x})$, and where L_{ij} is a difference approximation matrix to the operator $\partial_{x_i}^1 \left(g_i \partial_{x_i}^1 \partial_{x_j}^2\right)$. Unfortunately, this explicit scheme require very small time steps Δt in order to be stable. A possible amelioration consists on the use of a Du Fort and Frankel (FFD) scheme which is unconditionally stable but is no longer consistent for to large time steps Δt.

Additive Operator Splitting scheme. We can use an Additive Operator Splitting (AOS) scheme of the form

$$U^{k+1} = \frac{1}{2} \sum_{n=1}^{2} (I + 2\Delta t L_{nn})^{-1} \left(I - \Delta t \sum_{i=1}^{2} \sum_{j \neq i} L_{ij}\right) U^k. \tag{17}$$

This method presents better stability properties, but requires matrix inversions which come down to solving diagonally dominant pentadiagonal systems (for term with L_{nn}) of linear equations and can be performed with a modified Thomas algorithm [56]. We can note that in equation (17) matrices L_{nn} not depend on iteration k, so matrix inversions are then performed only one time at the beginning ($k = 0$) of the iterative scheme.

Alternate Direction Implicit scheme. In order to reduce complexity, a simplification can be performed on equation (15) which can be rewritten as

$$u_t = -\sum_{i,j=1}^{2} a_{ij} \partial_{x_i}^2 \partial_{x_j}^2 u - \sum_{i,j=1}^{2} b_{ii} \partial_{x_i}^1 \partial_{x_j}^2 u,$$

where $a_{ij} = \frac{1}{2}(g_i + g_j)$ and $b_{ii} = \partial_{x_i}^1 g_i$. As g_i is piecewise constant, terms in second summation can be neglected, approximated continuous formulation is then given by

$$u_t \approx -\sum_{i,j=1}^{2} a_{ij} \partial_{x_i}^2 \partial_{x_j}^2 u. \tag{18}$$

We therefore propose the use of Alternating Direction Implicit (ADI) type schemes (accurate to second order in time) which is extensively used for second-order diffusion equation. Fourth-order PDEs are more difficult to implement with ADI, as equation (18) includes a cross-term. Witelski and Bowen [57] suggest an ADI scheme in which the mixed derivative term is computed explicitly. Then equation (18) is numerically resolved as

$$U^{k+1} = \left(\prod_{n=1}^{2} (I - \Delta t A_{nn})\right)^{-1} \left(I + \Delta t \sum_{i=1}^{2} \sum_{j \neq i} A_{ij}\right) U^k, \tag{19}$$

where A_{ij} is a central difference approximation matrix to the operator $a_{ij} \partial_{x_i}^2 \partial_{x_j}^2$.

VI. Results

In this section, we firstly prove in subsection VI-A, the efficiency of the PDE interpolator by comparison with some existing methods. Secondly, in subsection VI-B, some experiments illustrate obtained results on various applications of the PDE-based BEMD.

A. PDE interpolator performance

The notion of (digital) image inpainting was first introduced in the paper of Bertalmio-Sapiro-Caselles-Ballester [63]. Smart digital inpainting models, techniques, and algorithms have broad applications in image interpolation, photo restoration, zooming and super-resolution, primal-sketch based perceptual image compression and coding, and the error concealment of (wireless) image transmission, etc.. Another approach uses ideas from classical fluid dynamics to propagate isophote lines continuously from the exterior into the region to be inpainted [68]. This method is directly based on the Navier-Stokes equations which was well-developed with theoretical and numerical results. Inspired by the work of Bertalmio et al., Chan and al. have proposed a general mathematical models for local inpainting of nontexture images. In the following, we made some experiments, only to show how the PDE interpolator works. Figure 5 shows an example of image inpainting and noise removal results on a degraded LENA image. Figures $5(c)$ and (f) show the original image, and Figures $5(d)$ and (g) are the occluded (degraded) image. The PDE-based Inpainting method consists to calculate the mean-envelope of degraded image. Here the diffusivity functions $g^{\pm}(x)$ are set to 1 on occlusion domain (triangular areas on Figures $5(d)$ and (g)) where lost data must be restored. Figures $5(e)$ and (h) illustrates the resulting restored image. Figure $5(a)$ illustrate Lena picture with 17,76 dB noise level and its restored version by PDE-interpolator with obtained Signal-to-Noise Ratio (SNR) equal to $21,88$ dB. On Figure $5(b)$, Lena picture with $13,83$ dB noise level is restored by PDE-interpolator with final SNR equal to $21,88$ dB.

This is not an easy task, if we know just little informations on an original image as some part of the features such as edges, and that we want to restore this incomplet image. In the example in Figure 1, degraded masks of 10%, 23% and 35% of the image are applied on. To restore these degraded images, we perform an inpainting operation through three different interpolation methods: Laplace, k - Neighbors (kNN) (with $k = 4$ or 6) and our PDE-interpolator. By comparing the Signal-to-Noise Ratio (SNR), the obtained results show that the PDE-interpolator works better than the others two methods. To complete the demonstration with the SNR, a zoom on the results in figure1(d) is performed for more visual appreciation.

In Figure 2, only 50%, 23%, 35% and 5% of the image is alternately available. From these informations, we perform an restoration of the incomplet images by different methods: Laplace, k-Nearest neighbor and our PDE-interpolator. By comparing the Signal-to-Noise Ratio, the obtained results show that the PDE-interpolation works better than the others. In the case of 5% for example, PDE-interpolator is far better considering the SNR and the visual quality of the image result.

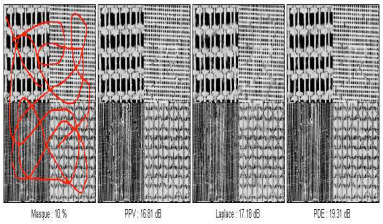

(a) Inpainting on Brodatz with 10% of pixels masked

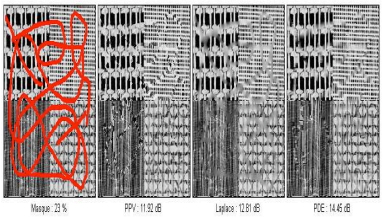

(b) Inpainting on Brodatz with 23% of pixels masked

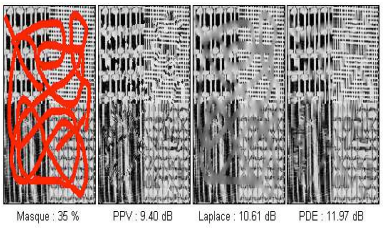

(c) Inpainting on Brodatz with 35% of pixels masked

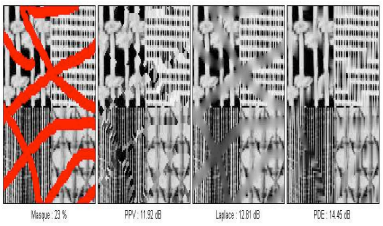

(d) Zoom on Brodatz at 23%

Fig. 1. Illustration of image inpainting using PDE-interpolator: Visual comparaison of PDE-interplator, kNN and Laplace methods.

B. Some applications of PDE-based BEMD

In these experiments, several synthetic and real images are used to test effectiveness of our approach. We recall that in PDE-based EMD, the same stopping criteria as in the classical BEMD algorithm [23] are used.

In this section we are interesting on various possible applications of BEMD, such as texture extraction, image denoising or image inpainting. Particulary, in image segmentation problems, texture extraction is a crucial step and is one of the most important techniques for image analysis and understanding. One of the crucial aspects of texture analysis is the extraction of textural features and properties. The use of filter operators has been applied successfully to a variety of computer vision problems. A set of linear or non-linear operators is generally applied to the

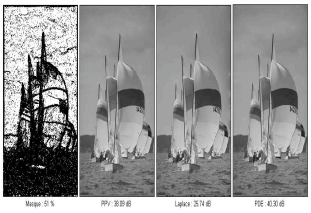

(a) Image restauration of Boat with 50% of the total information

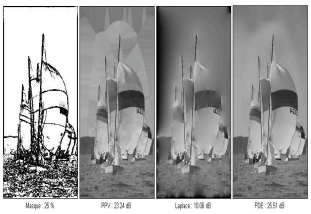

(b) Image restauration of Boat with 25% of the total information%

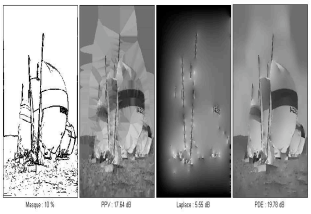

(c) Image restauration of Boat with 35% of the total information

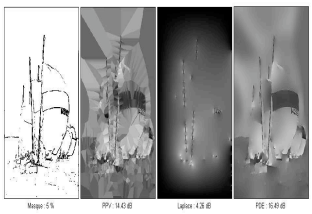

(d) Image restauration of Boat with 5% of the total information

Fig. 2. Illustration of image restauration using PPV, Laplace and PDE-interpolator: in case of 5%, even if their SNR are similar, the visual quality of PDE-interpolator is obvious with respect to Laplace result which is work more than kNN method.

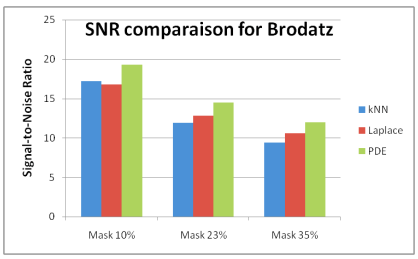

Fig. 3. Comparaison of Signal-to-Noise Ratio in brodatz image test. A qualitative comparaison beetwen PDE-interpolator, kNN and Laplace Methods. PDE-interpolator yield better results in image restoration.

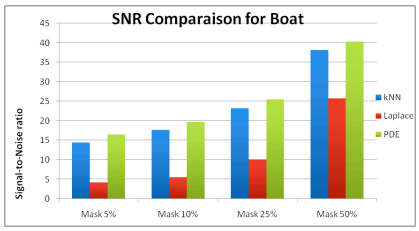

Fig. 4. Comparaison of Signal-to-Noise Ratio in bottle image test. A qualitative comparaison beetwen PDE-interpolator, kNN and Laplace Methods. PDE-interpolator yield better results in image reconstruction.

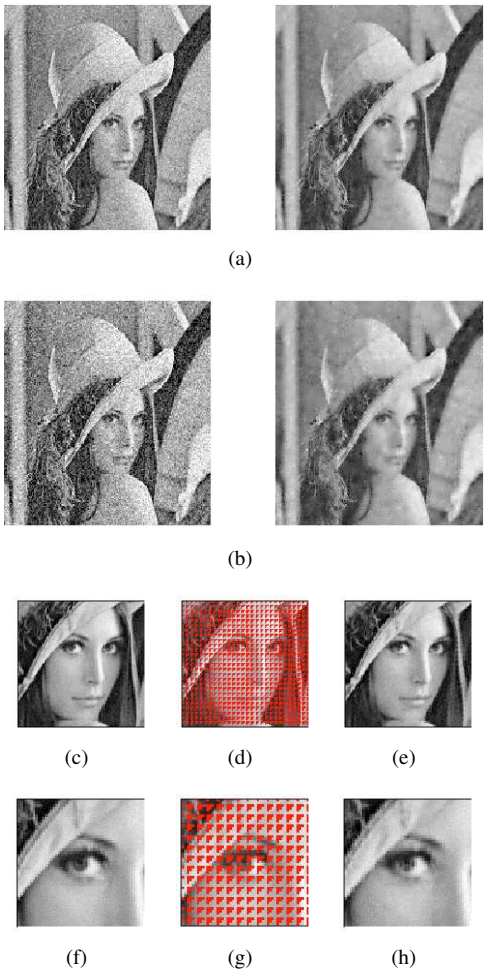

(a) (b) (c) (d) (e) (f) (g) (h)

Fig. 5. Image inpainting and Restoration examples on 'LENA' image. (a) Noised Lena with 17,76 dB and the restored version with PDE-interpolator (21,88 dB). (b) Noised Lena with 13,83 dB and the restored version with PDE-interpolator (19,75 dB).(c) Original image. (d) Degraded image. (e) Inpainting result image. (f)-(g) Zoom on for images (c)-(e).

input image, that creates a multimodal data space. There is a lot of related work on the optimal filter selection for texture segmentation. Most of approaches adopt predefined filter bank that is composed of isotropic or anisotropic filters such as the Gaussian operator, the Laplacian-of-Gaussian operator [58], or the 2D Gabor operators with different scale and orientation [59]–[61]. An alternative selection is the wavelet transform, which provides a unifying framework for the analysis and characterization of an image into different scales (see for example [62]).

First example (oriented decomposition). To compare the effect of the selective directional diffusion, we implement equation (11) by splitting directions, $(X, Y) = (x_1, x_2)$. Figure 6 illustrates the decomposition of a synthetic image composed of FM components, figure $6(a)$. Figures $6(b) - (c)$ show respectively first IMF and residual obtained in X-direction. Figures $6(d) - (e)$ show respectively first IMF and residual obtained in Y-direction. Figures $6(f) - (g)$ show respectively first IMF and residual obtained in both X- and Y-direction. Finally, figures $6(h) - (i)$ show respectively first IMF and residual obtained in Y-direction after diffusion in X-direction, resulting on extraction of IMF in diagonal direction.

Second example (adaptive decomposition). Figure 8, is a comparison between BEMD and Laplacian pyramid [58] for hight frequencies components extraction. The original image, figure $8(a)$, is decomposed in a hight frequencies component image, figure$8(b)$, and a residual image, figure $8(d)$ with BEMD approach. The decomposition obtained with Laplacian pyramid no permits catching of all strips of zebra, see figure $8(c)$ for hight frequencies component (Laplacian) image and figure $8(e)$ for residual (Gaussian) image.

Third example (extracting features, structure and texture). Figure 9 show how BEMD can extract multi-oriented texture without introducing smoothing effect. Figure $9(b)$ and figure $9(c)$ show respectively the first IMF (texture image) and the residual (structure image) of BARBARA original image, figure $9(a)$.

Fourth example (image denoising). Figure 7 shows how BEMD can acts as a denoising filter. An initial image, figure $7(a)$, is corrupted with Gaussian noise, Figure $7(b)$. The fifth IMF corresponds to the denoised image, figure $7(c)$.

Fifth example (texture analysis). Figure 10 shows PDE-BEMD for a direct texture analysis. An initial image, figure $10(a)$, is decomposed into IMFs, Figure $10(b - c - d)$ and an residual component in $10(e)$. For color images decomposition, the PDE-based BEMD method is applied for each color plane. In the principle, it can be compared to multidimensional EMD implementation as presented in [69], where a set of common frequency scales can be determined by simultaneously decomposing sources using the bivariate EMD.

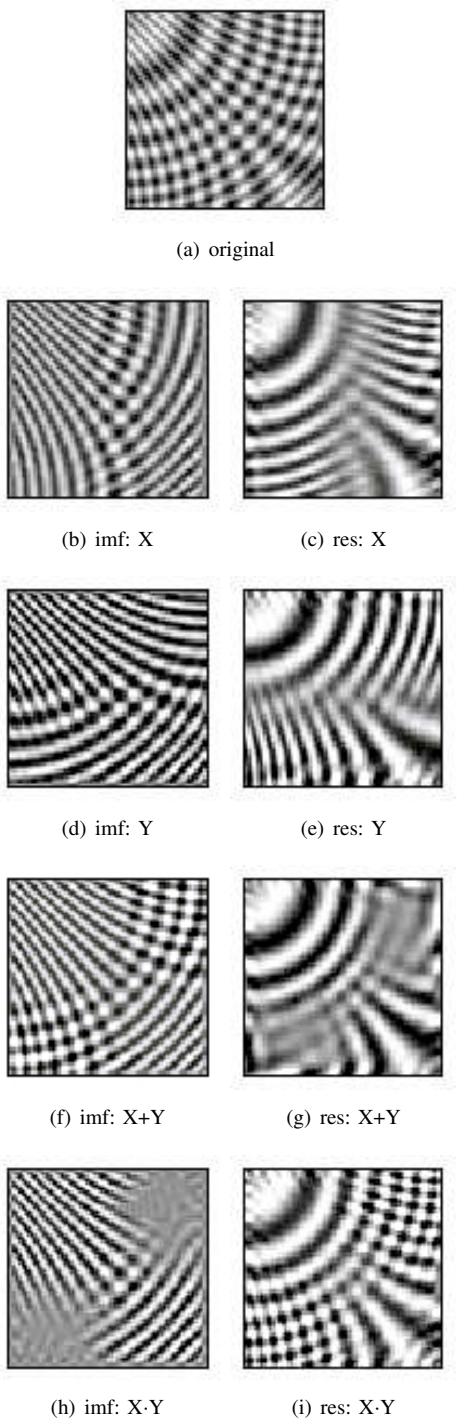

(a) original

(b) imf: X (c) res: X

(d) imf: Y (e) res: Y

(f) imf: X+Y (g) res: X+Y

(h) imf: X·Y (i) res: X·Y

Fig. 6. Illustration of the directional and local adaptative frequency decomposition for PDE-based BEMD. (a) Original multicomponent FM image. (b)-(c) First IMF and residual for decomposition in column direction (X). (d)-(e) First IMF and residual for decomposition in row direction (Y). (f)-(g) First IMF and residual for decomposition in both directions (X+Y). (h)-(i) First IMF and residual for decomposition in row direction following by decomposition in column direction (X·Y).

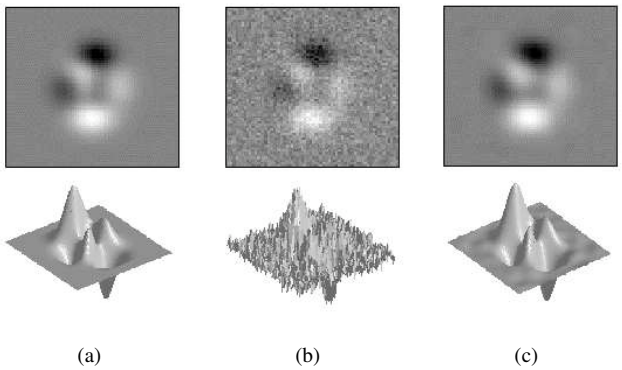

Fig. 7. Illustration of image denoising using PDE-based EMD. (a) Free-noise image, 2D (up) and surface (down) representations. (b) Same as in (a) with additive Gaussian noise. (c) The denoised image is given by the fifth IMF.

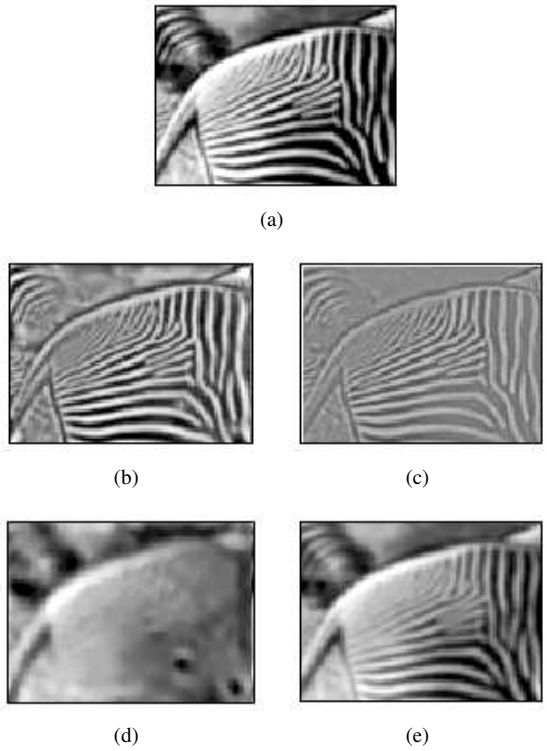

Fig. 8. Comparison between PDE-based BEMD and Laplacian Pyramid approach. (a) Original image. (b) and (d) first IMF and residual of BEMD. (c) and (e) First level of Laplacian and Gaussian pyramids. Whereas BEMD is able to extract a broad band FM component, Laplacian decomposition failed. All strips of zebra are identified in first IMF (b), but only high frequency strips are catching in (c).

VII. Conclusion

In this paper, we have proposed an 2D PDE-based version to the purely algorithmic implemented sifting process used in the original Huang's EMD method. The approach to solve the selective signal smoothing is based on a fourth-order nonlinear diffusion equation. In the spirit of the original sifting process, this nonlinear filtering algorithm is equivalent to an iterated sequence of regularization and reconstruction processes. Experimental results show that our approach can be used to achieve signal decomposition with a valuable

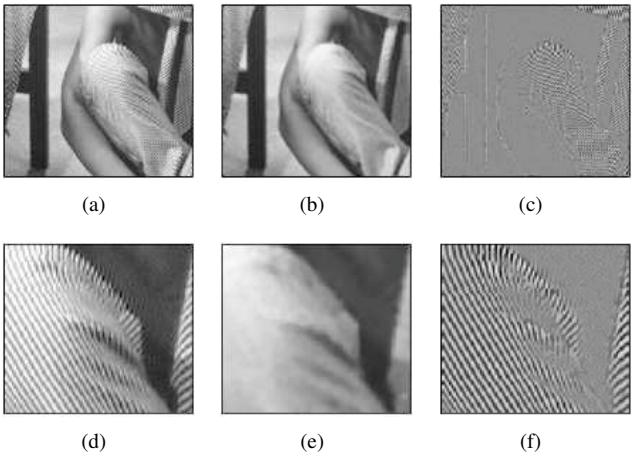

Fig. 9. Illustration of BEMD-based image filtering on 'BARBARA' image. (a) Original image. (b) and (c) approximation (residual) image and details (first IMF) image. (d)-(f) Closed-up on images (a)-(c).

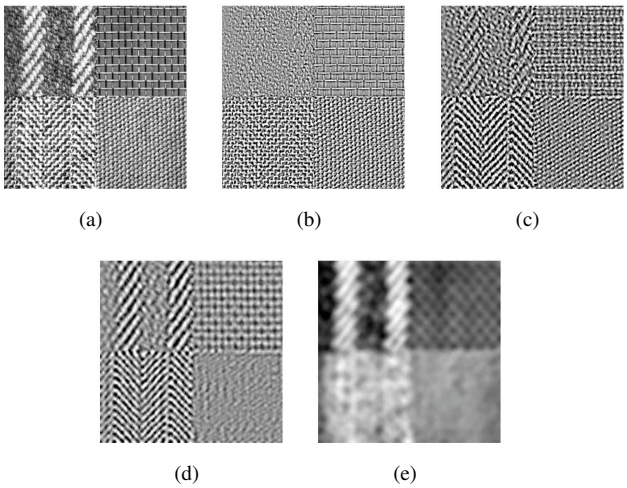

Fig. 10. Illustration of PDE-Based BEMD texture on 'Brodatz' image. (a) Original image. (b - c and d) details with succesive IMFs from PDE-BEMD. (e) the residu of the EMD.

performance. Especially in the case of images, the method is very efficient and time consuming competitive compared to existing 2D version of EMD in the literature like RBF-tools that we used in previous works for BEMD implementation. The main contribution of this paper was the use of 2D PDE-interpolator that works like a selective image smoothing method. In accordance with the analytical approach for sifting process depicted in previous works, this method can be used for extracting transient signal and for intermittencies removal problems. Finally the 2D version of this approach could boost applications of EMD in image analysis and compression which is the subject of ongoing work.

References

[1] O. Niang,E. Deléchelle and J. Lemoine," An Spectral approach for sifting process in Empirical Mode Decomposition," IEEE Transaction on Signal Processing, vol.58, num 11, pp. 5612-5623, 2010.

[2] O. Niang, "Empirical Mode Decomposition: Contribution à la modélisation mathématique et application en traitement du signal et l'image," PhD thesis, Univ Paris 12, Créteil, France, Septembre 2007.

[3] E. Deléchelle, J. Lemoine, and O. Niang, "Empirical Mode Decomposition: An Analytical Approach for Sifting Process," IEEE Signal Processing Letters, vol. 12, num 11, pp. 764-767, 2005.

[4] N. E. Huang, Z. Shen, S. R. Long, M. L. Wu, H. H. Shih, Q. Zheng, N. C. Yen, C. C. Tung, and H. H. Liu, "The empirical mode decomposition and Hilbert spectrum for nonlinear and non-stationary time series analysis," Proc. Roy. Soc. London A, vol. 545, pp. 903-995, 1998.

[5] K. T. Coughlin and K. K. Tung, "The 11-year solar cycle in the stratosphere extracted by the empirical mode decomposition method," Adv. Space Res., vol. 34, pp. 323-329, 2004.

[6] R. Fournier, "Analyse stochastique modale du signal stabilométrique. Application à l'étude de l'équilibre chez l'Homme." Créteil (France): Thèse de doctorat, Univ. Paris XII Val-de-Marne, 2002.

[7] E. P. Souza Neto, M.-A. Custaud, C. J. Cejka, P. Abry, J. Frutoso, C. Gharib, and P. Flandrin, "Assessment of cardiovascular autonomic control by the Empirical Mode Decomposition," 4th Int. Workshop on Biosignal Interpretation, Como (Italy), 2002.

[8] Z. Wu, E. K. Schneider, Z. Z. Hu, and L. Cao, "The impact of global warming on ENSO variability in climate records," COLA Technical Report CTR 110, October 2001.

[9] P. Flandrin, http://www.ens-lyon.fr/ flandrin/software.html.

[10] Norden Huang and al., http: //rcada.ncu.edu.tw/research1 clip ex.htm.

[11] E. Deléchelle, http://perso.wanadoo.fr/e.delechelle/codes.html.

[12] G. Rilling, P. Flandrin, and P. Gonçalvès, "On Empirical Mode Decomposition and its Algorithms," presented at IEEE-EURASIP Workshop on Nonlinear Signal and Image Processing NSIP-03, Grado (Italy), 2003.

[13] P. Flandrin, G. Rilling, and P. Gonçalvès, "Empirical mode decomposition as a filter bank," IEEE Signal Processing Letters, vol. 11, pp. 112-114, 2004.

[14] P. Flandrin and P. Gonçalvès " Empirical Mode Decompositions as Data-Driven Wavelet-Like Expansions," Int. Journal of Wavelets, Multires. and Info. Proc., to appear, 2004.

[15] P. Flandrin, P. Gonçalvès, and G. Rilling, "EMD Equivalent Filter Banks, from Interpretation to Applications," in Hilbert-Huang Transform: Introduction and Applications, S. S. P. Shen, Ed.: World Scientific, 2004.

[16] P. Flandrin, "Some aspects of Huang's Empirical Mode Decomposition, from interpretation to applications," Int. Conf. on Computational Harmonic Analysis CHA-04 (invited talk), Nashville (TN), 2004.

[17] Z. Wu and N. E. Huang, Ensemble empirical mode decomposition: A noise-assisted data analysis method, Adv. Adapt. Data Anal. 1 (2009) 141.

[18] Wu ZH, Huang NE, Chen XY (2009) The Multi-Dimensional Ensemble Empirical Mode Decomposition Method. Adv Adaptive Data Anal 1: 339372.

[19] Toshihisa Tanaka and Danilo P. Mandic, "Complex Empirical Mode Decomposition", IEEE Signal Processing Letters, VOL. 14, NO. 2, pp.101-104, February 2007.

[20] M. U. B. Altaf, T. Gautama, T. Tanaka, and D. P. Mandic, "Rotation invariant complex empirical mode decomposition," in Proc. Int.Conf. Acoustics, Speech, Signal Processing (ICASSP), 2007, vol. 3, pp.10091012.

[21] G. Rilling, P. Flandrin, P. Goncalves, and J. Lilly, "Bivariate empirical modedecomposition," IEEESignal ProcessingLetters, vol. 14, no. 12, 2007.

[22] J. Fleureau, J.C. Nunes, A. Kachenoura, L. Albera and L. Senhadji , "Turning Tangent Empirical Mode Decomposition: A framework for mono- and Multivariate Signals", IEEE Transactions on signal Processing, vol. 59, n3, march 2011.

[23] J.-C. Nunes, Y. Bouaoune, E. Deléchelle, O. Niang, and Ph. Bunel, "Image analysis by bidimensional empirical mode decomposition," Journal of Image and Vision Computing, vol. 21, pp. 1019-1026, 2003.

[24] J.-C. Nunes, S. Guyot, and E. Deléchelle, "Texture analysis based on the bidimensional empirical mode decomposition," Journal of Machine Vision and Applications, 2005.

[25] C. Damerval, S. Meignen, and V. Perrier,"A fast algorithm for bidimensional emd,"IEEE Signal Processing Letters, vol. 12, no. 10, pp. 701-704, October 2005.

[26] Y. Xu, B. Liu, J. Liu, and S. Riemenschneider, "Two- dimensional empirical mode decomposition by finite elements,"The Royal Society A, pp. 1-17, 2006.

[27] S. M. A. Bhuiyan, R. R. Adhami, and J. F. Khan, "A novel approach of fast and adaptative bidimensional empirical mode decomposition," in IEEE ICASSP, 2008, pp. 1313-1316.

[28] Sharif M. A. Bhuiyan, Reza R. Adhami, and Jesmin F. Khan," Fast and Adaptive Bidimensional Empirical Mode Decomposition Using Order-Statistics Filter Based Envelope Estimation," in EURASIP Journal on Advances in Signal Processing, article ID 728356, 2008.

[29] N. Rehman and D. P. Mandic, " Multivariate empirical mode decomposition," in Proc. R. Soc. A (2010) 466, 12911302.

[30] G. Jager, R. Koch, A. Kunoth, R. Pabel, Fast Empirical Mode Decompositions of Multivariate Data Based on Adaptive Spline-Wavelets and a Generalization of the Hilbert-Huang-Transform (HHT) to Arbitrary Space Dimensions, Advances in Adaptive Data Analysis (AADA) 2(3), 2010, 337-358.

[31] Norden R Huang and al. http://rcada.ncu.edu.tw/research1.htm

[32] Gabriel Rilling and Patrick Flandrin,"On the influence of sampling on the empirical mode decomposition ", IEEE, ICASSP, 2006.

[33] Zhengguang Xu, Benxiong Huang, and Fan Zhang,"Improvement of empirical mode decomposition under low sampling rate," Signal processing, Vol.89, n11, pp. 2296-2303, 2009.

[34] Zhengguang Xu, Benxiong Huang, and Kewei Li, "An alternative envelope approach for empirical mode decomposition ," Digital Signal Process, elsevier, Vol.20, pp. 77-84, 2010.

[35] Ingrid Daubechies , Jianfeng Lu1 and Hau-Tieng Wu, "Synchrosqueezed Wavelet Transforms: an Empirical Mode Decomposition-like Tool". Preprint submitted to Applied and Computational Harmonic Analysis July 25, 2010.

[36] V. Vatchev, "Analysis of Empirical Mode Decomposition Method," presented at USC, 2002.

[37] Oumar Niang, Mouhamed Ould Guerra, Abdoulaye Thioune, Eric Deléchelle, Mary Teuw Niane and Jacques Lemoine,"A propos de l'Orthogonalit dans la Dcomposition Modale Empirique". Conference GretSI 2011, Bordeaux, Septembre 2011.

[38] J. D. Murray, *Mathematical Biology*, vol. 19. Berlin Heidelberg New-York: Springer-Verlag, 1993.

[39] F. Catté, P. L. Lions, J. M. Morel, T. Coll, "Image selective smoothing and edge detection by nonlinear diffusion," SIAM J. Numer. Anal. vol. 129, pp. 182-193, 1992.

[40] P. Perona, J. Malik, "Scale-space and edge detection using anisotropic diffusion", IEEE Trans. On Pattern Analysis and Machine Intelligence, vol. 12(7), pp. 629-639, 1990.

[41] Y. Meyer, "Oscillating Patterns in Image Processing and Nonlinear Evolution Equations" Univ. Lecture Ser. 22, AMS, Providence, RI, 2002.

[42] S. Osher, A. Sole and L. Vese, "Image decomposition and restoration using total variation minimization and the H^1 norm Multiscale Modeling and Simulation". A SIAM Interdisciplinary Journal, 1(3), 2003, pp. 349 - 370.

[43] M. Lysaker, A. Lundervold, and X.-C. Tai, "Noise Removal Using Fourth-Order PartialDifferential Equations with Applications to Medical Magnetic Resonance Images in Space and Time", IEEE Trans. On Image Processing, Vol. 12, No. 12, December 2003.

[44] J. Weickert, B. M. ter Haar Romeny, and M. Viergever, "Efficient and Reliable Schemes for Nonlinear Diffusion Filtering," IEEE Trans. On Image Processing, vol. 7, pp. 398, 1998.

[45] J. Weickert, "A review of nonlinear diffusion filtering," in Scale-Space Theory for Computer Vision, vol. 1252, Lecture Notes in Computer Science, B. H. Romeny, Ed. New York: Springer, 1997, pp. 3-28.

[46] D. W. Peaceman and H. H. Rachford, "The Numerical Solution of Parabolic and Elliptic Differential Equations," Journal Soc. Ind. Appl. Math., vol. 3, pp. 28, 1955.

[47] D. Barash and R. Kimmel, "An Accurate Operator Splitting Scheme for Nonlinear Diffusion Filter," HP Company 2000.

[48] A. Chun-Chieh Shih, H.-Y. M. Liao, and C.-S. Lu, "A New Iterated Two-Band Diffusion Equation: Theory and Its Application," IEEE Trans. On Image Processing, vol. 12, 2003.

[49] A. Chambolle and P.-L. Lions, "Image recovery via total variation minimization and related problems," Numer. Math., vol. 76, pp. 167-188, 1997.

[50] T. Chan, A. Marquina, and P. Mulet, "High order total variation-based image restoration," SIAM J. Sci. Comp., vol. 22, pp. 503-516, 2000.

[51] M. Lysaker, S. Osher, and X.-C. Tai, "Noise removal using smoothed normals and surface fitting," UCLA CAM preprint 03-03, 2003.

[52] J. Tumblin and G. Turk, "LCIS: A boundary hierarchy for detail-preserving contrast reduction," SIGGRAPH 1999 annual conference on Computer Graphics, Los Angeles, CA USA, 1999.

[53] G. W. Wei, "Generalized Perona-Malik equation for image processing," IEEE Signal Processing Letters, vol. 69, pp. 165-167, 1999.

[54] Y.-L. You and M. Kaveh, "Fourth order partial differential equations for noise removal," IEEE Trans. On Image Process., vol. 9, pp. 1723-1730, 2000.

[55] J. Tumblin, *private communication*, 2003.

[56] G. Engeln-Muellges and F. Uhlig, in Numerical Algorithms with C, Chapter 4., Springer-Verlag Berlin, 1996.

[57] T.P. Witelski and M. Bowen. "ADI schemes for higher-order nonlinear diffusion equations," Appl. Numer. Math., 45(2-3), pp. 331-351, 2003.
[58] P. J. Burt, E. H. Adelson, "The Laplacian Pyramid as a Compact Image Code," IEEE Trans. on Communications, pp. 532–540, April 1983.
[59] D. Gabor, Theory of communications. IEE proceedings, 93, 1946.
[60] A. Bovik, M. Clark, and W. Geister, "Multichannel texture analysis using localized spatial filters," IEEE Transactions on Pattern Analysis and Machine Intelligence, vol. 12, pp. 55-73, 1990.
[61] D. Dunn and W. Higgins, "Optimal Gabor filters for texture segmentation," IEEE transactions on Image Processing, vol. 4, pp. 947-964, 1995.
[62] M. Unser, "Texture classification and segmentation using wavelet frames," IEEE Transactions on Image Processing, vol. 4, pp. 1549-1560, 1995.
[63] M. Bertalmio, G. Sapiro, V. Caselles, and C. Ballester. "Image inpainting," Computer Graphics, SIGGRAPH 2000, July, 2000.
[64] P. Mrázek, J. Weickert, G. Steidl, and M. Welk. "On Iterations and Scales of Nonlinear Filters," Proc. of the Computer Vision Winter Workshop, ed.:O. Drbohlav, Valtice, Czech Republic, pp. 61-66, Feb. 3-6, 2003.
[65] M. Unser, A. Aldroubi, and M. Eden, "The L_2 Polynomial Spline Pyramid," IEEE Trans. On Pattern Analysis and Machine Intelligence, vol. 15(4), pp. 364-379, April 1993.
[66] T. F. Chan and J. Shen, "Mathematical models of local non-texture inpaintings", SIAM J. Appl. Math, 62(3):10191043, 2002.
[67] L. Rudin, S. Osher, and E. Fatemi, "Nonlinear total variation based noise removal algorithms" Phys. D, 60 (1992), pp. 259268.
[68] M. Bertalmio, A. L. Bertozzi, and G. Sapiro, "Navier-Stokes, Fluid Dynamics, and Image and Video Inpainting", Proceedings of the International Conference on Computer Vision and Pattern Recognition, IEEE, Dec. 2001, Kauai, HI, volume I, pp. I-355-I362.
[69] Looney, D. and Mandic, D. P, "Multiscale image fusion using complex extensions of EMD". IEEE Trans. Signal Process, 2009. 57, 16261630.

Oumar Niang received the Ph.D. degree in computer sciences - actual biomedical engineering - from the Laboratoire Images, Signaux et Systèmes Intelligents (LISSI-E.A. 3956), Université Paris Est Créteil Val-de- Marne- ex Paris 12 Val–de–Marne - , Créteil, France, in 2007. He is a Rechearch Professor at the Ecole Polytechnique de Thies Sénégal. He is member of Laboratoire d'Analyse Numérique et d'Informatique (LANI) UGB Sénégal with research interests focused on mathematical modeling in signal processing, images processing and complex systems, time frequency analysis, biomedical signal and medical image analysis.

Abdoulaye Thioune received the master thesis in Transmission de Données et Sécurité de l'Information at Laboratoire d'Algèbre, de Cryptologie, de Géométrie Algébrique et Applications de la faculté des Sciences et Technique, Université Cheikh Anta Diop de Dakar Sénégal, in 2009. He prepare actually the Phd degree in biomedical engineering at the Laboratoire Images, Signaux et Systèmes Intelligents (LISSI-E.A. 3956), Université Paris 12 Val–de–Marne, Créteil, France.

Mouhamed Cheikh El Gueirea He received the master thesis at UFR Sciences Appliquées et de Technologie de l'Université Gastion Berger (UGB) de Saint-Louis, and is member of Laboratoire d'Analyse Numérique et d'Informatique (LANI) UGB Sénégal, in 2007. He prepare actually the Phd degree in Numerical Analysis at the same university.

Éric Deléchelle received the Ph.D. degree in biomed- ical engineering from the Université Paris Est Créteil Val-de-Marnel, France, in 1997. He is with the Laboratoire Images, Signaux et Systèmes Intelligents (LiSSi-EA 3956), Université Paris 12 Val-deMarne, Créteil. Since 1999, he has been Maitre de Conférences at the Institut Universitaire de Technologie, Créteil, with research interests focused on stochastic signal analysis, biomedical signal, and medical image processing.

Jacques Lemoine received the Ph.D. degree in biomedical engineering from the Université Paris Est Créteil Val-de-Marnel, France, in 1981. He is a Distinguished Professor in the Laboratoire Images, Signaux et Systèmes Intelligents (LiSSi-EA 3956), UFR des Sciences et Technologie, Université Paris Est Créteil Val-de-Marne, France. His research interests are focused on stochastic signal analysis, biomedical signal, and medical image processing.